Received: 12 December 2019 | Revised: 13 February 2020 | Accepted: 13 February 2020
DOI: 10.1002/jrs.5860

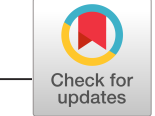

RESEARCH ARTICLE

Temperature dependence of strain–phonon coefficient in epitaxial Ge/Si(001): A comprehensive analysis

C.L. Manganelli[1] | **M. Virgilio**[2] | **O. Skibitzki**[1] | **M. Salvalaglio**[1,3,4] | **D. Spirito**[1] | **P. Zaumseil**[1] | **Y. Yamamoto**[1] | **M. Montanari**[5] | **W.M. Klesse**[1] | **G. Capellini**[1,5]

[1]IHP–Leibniz-Institut für innovative Mikroelektronik, Material Research-Semiconductor Optoelectronics, Frankfurt (Oder), Germany
[2]Dipartimento di Fisica, Università di Pisa, Pisa, Italy
[3]Institut für Wissenschaftliches Rechnen, Technische Universität Dresden, Dresden, Germany
[4]Dresden Center for Computational Material Science, Technische Universität Dresden, Dresden, Germany
[5]Dipartimento di Scienze, Università degli Studi Roma Tre, Roma, Italy

Correspondence
Costanza Lucia Manganelli, IHP–Leibniz-Institut für innovative Mikroelektronik, Im Technologiepark 25, D-15236 Frankfurt (Oder), Germany.
Email: manganelli@ihp-microelectronics.com

Funding information
Horizon 2020 Framework Programme, Grant/Award Number: 766719

Abstract

We investigate the temperature dependence of the Ge Raman mode strain–phonon coefficient in Ge/Si heteroepitaxial layers. By analyzing the temperature-dependent evolution of both the Raman Ge—Ge line and of the Ge lattice strain, we obtain a linear dependence of the strain–phonon coefficient as a function of temperature. Our findings provide an efficient method for capturing the temperature-dependent strain relaxation mechanism in heteroepitaxial systems. Furthermore, we show that the rather large variability reported in the literature for the strain–phonon coefficient values might be due to the local heating of the sample due to the excitation laser used in μ-Raman experiments.

KEYWORDS

Germanium, temperature-dependent, strain, phonon coefficient, epitaxial layers, HR-XRD

1 | INTRODUCTION

In the last decade, the optical emission properties of heteroepitaxial Ge/Si have been thoroughly investigated in view of completing the silicon photonic platform with an integrated light emitter devices based on this material system.[1–7] A popular strategy adopted to improve the radiative recombination efficiency of Ge layers is based on tensile lattice strain. Indeed, this mechanical deformation of the lattice can lead to a direct band gap material. This aim has been pursued by different approaches such as the epitaxial growth on suitable buffer layers,[8] the use of external stressors,[9,10] micromachining,[11] and the control of the plastic relaxation processes of the heteroepitaxial strain.[12,13] Similarly, lattice straining has also been investigated as a route to boost the performances of field effect transistor devices based on epitaxial Ge, through its beneficial impact on the carrier mobility,[14] and understand their structural stability.[15]

This is an open access article under the terms of the Creative Commons Attribution-NonCommercial License, which permits use, distribution and reproduction in any medium, provided the original work is properly cited and is not used for commercial purposes.
© 2020 The Authors. Journal of Raman Spectroscopy published by John Wiley & Sons Ltd

In this framework, the accuracy of strain measurements in Ge/Si heterostructures, possibly with high spatial resolution, is of great relevance. Spatially-resolved strain measurements are routinely carried out through micro-Raman spectroscopy, which is a versatile and noninvasive technique. It measures the shift of the phonon modes induced by strain and composition. Strain determination is nondirect because it relies on material parameters determined by other experimental techniques. The relation between the Raman wavenumber shift $\Delta\omega$ of a phonon active mode associated to a strain field of magnitude ε is given by a phenomenological strain–phonon coefficient (or phonon strain–shift coefficient)

$$b = \frac{\Delta\omega}{\varepsilon} \quad (1)$$

In the following, we will consider the case of biaxial strain, typical for heterostructures. In the case of Ge/Si heterostructures, the values of b reported in literature are quite scattered (see Table I in the following) thus limiting the reliability of this technique. Furthermore, to the best of our knowledge, the strain–phonon coefficient has been so far only determined at room temperature (RT) albeit the disentanglement of the strain and temperature effects in Raman spectroscopy has recently gained attention.[16,17] The need of reliable reference parameters can be better appreciated considering that the knowledge of the T-dependence of b, and $b(T)$, is essential to investigate the strain relaxation mechanisms of Ge/Si heterostructures, usually grown in the 800–1,200 K range and cooled down at room or cryogenic temperatures for optical measurements.[18,19] Furthermore, we notice that the knowledge of $b(T)$ can be beneficial for the interpretation of Raman spectra collected at different laser pump powers, allowing for a better assessment of local heating effects.[20]

In this paper, we investigate the temperature dependence of the strain–phonon coefficient of Raman modes in epitaxial Ge/Si layers. To this aim, we first describe theoretically how $b(T)$ is linked to the temperature dependence of the material elastic constants and the phonon wavenumber. Subsequently, we analyze the biaxial strain field as a function of T, explicitly evidencing that $\varepsilon(T)$ can be decomposed into two separate contributions: (a) the epitaxial strain, due to the Si—Ge lattice mismatch (at a specific temperature), and (b) the thermal strain, caused by the difference between the coefficient of thermal expansion (CTE) of the Ge epilayer and the relatively thick Si substrate. Finally, we use these results to directly extract the $b(T)$ in Ge/Si samples in the 150–450 K range, by comparing T-dependent μ-Raman measurements with T-dependent high-resolution X-ray diffraction experiments (HR-XRD), a method that can be readily generalized to a large class of semiconductor layers.

2 | TEMPERATURE DEPENDENCE OF THE RAMAN SHIFT AND OF THE STRAIN FIELD

In this section, we shall discuss the temperature dependence of the elastic constants (in the Ge epilayer), of the Raman mode wavenumber, and of the lattice strain field on the measured Raman spectra.

In a diamond crystal lattice, as for Ge and Si, the Raman active modes are threefold degenerate at $k = 0$. This degeneration can be (at least partially) lifted by straining the lattice, thus lowering the crystal symmetry. The influence on the unstrained Raman wavenumber ω_0 of the different strain components ε_{ij} (with $i,j = x,y,z$, parallel to the three [001]-equivalent directions) can be derived through a first-order perturbation approach supported by group theory considerations (see Reparaz et al.[21] details are given in the Supporting Information, Note S1). In the backscattering geometry used in the present work, the only Raman mode observable is the longitudinal optical mode. It has a wavenumber given by

$$\omega = \omega_0 + \frac{q\left(\varepsilon_{xx} + \varepsilon_{yy}\right) + p\varepsilon_{zz}}{2\omega_0} \quad (2)$$

where p and q are the phonon deformation potentials (PDPs). In the case of heteroepitaxial layers, featuring a biaxial strain $\varepsilon_{bi} = \varepsilon_{xx} = \varepsilon_{yy}$ and $\frac{\varepsilon_{zz}}{\varepsilon_{bi}} = -\frac{2C_{12}}{C_{11}}$, we obtain

$$\Delta\omega = \omega - \omega_0 = \frac{\left(q - p\frac{c_{12}}{c_{11}}\right)\varepsilon_{bi}}{\omega_0} = b\,\varepsilon_{bi} \quad (3)$$

where we write the strain–phonon coefficient b as a function of the elastic constants c_{11} and c_{12} and of the PDPs.

As for the strain–phonon coefficient b, also the values of the PDPs in the literature are quite scattered.[21–25] Moreover, the ab initio calculations on Si with the use of a modified Keating's model for the valence force field[26–28] failed to reproduce experimental results. Another possible approach, not reproducible in this setup, is the fit of experimental measurements with the use of several empirical parameters and with a control on stress given by piezo-Raman measurements.[29] For Si and Ge (see for instance Rucker and Methfessel[30]), the temperature-dependence of the PDPs is not considered. Recent research activities on power-dependent Raman spectroscopy[20] analyze sets of previously published PDPs but neglect their temperature or power dependencies.

In analogy with these previous studies, we consider the approximation of PDPs quite insensitive to temperature variations and the dependence of $b(T)$ on T as due to T-induced evolution of the ratio between the elastic constants, given in Figure S1 according to McSkimin,[31] and of the Raman shift $\omega_0(T)$. By modeling this latter quantity taking into account T-induced effects on the lattice parameter, the phonon density of states, and the phonon decay rates associated to anharmonic terms in the ionic interaction potential, Safran et al.[32] and Burke et al.[33] have estimated a decrease of $\omega_0(T)$ characterized by a slope of $d\omega_0/dT = -0.02\ \text{cm}^{-1}/\text{K}$.

To capture the full impact of T on the Raman shift, we now discuss the T-dependence of the biaxial strain ε_{bi} due to the difference in the CTE of the substrate and epilayer. Following Isa et al.[13] we can express the lattice parameter of the substrate S and the layer L as

$$a_i(T) = a_i(T_0)\left[1 + \int_{T_0}^{T} \alpha_i(T')dT'\right] \tag{4}$$

where α_i is the T-dependent CTE with $i = S, L$, T is the measurement temperature, and T_0 is the highest temperature experienced by the sample during its deposition/annealing process, that is, the temperature at which the heteroepitaxial system forms.

The biaxial strain at a generic T, here defined as $\varepsilon_{bi}(T) = (a_L - a_S)/a_L$, is then given by:

$$\varepsilon_{bi}(T) = \frac{a_L(T_0)\left(1 + \int_{T_0}^{T} \alpha_L(T')dT'\right) - a_S(T_0)\left(1 + \int_{T_0}^{T} \alpha_S(T')dT'\right)}{a_L(T_0)\left(1 + \int_{T_0}^{T} \alpha_L(T')dT'\right)}$$
$$\approx \frac{a_L(T_0) - a_S(T_0)}{a_L(T_0)} + \int_{T_0}^{T} [\alpha_S(T') - \alpha_L(T')]dT' = \varepsilon_{bi}(T_0) + \varepsilon_{bi}^{th}(T) \tag{5}$$

where we assume that $\frac{a_S(T)}{a_L(T)} \approx 1$ and $\int_{T_0}^{T} \alpha_L(T')dT' \ll 1$, as it happens for Ge/Si material systems, and we neglect second-order corrections. It follows that, in agreement with Etzeldorfer et al.[25] the total strain results from the contribution of the heteroepitaxial term $\varepsilon_{bi}(T_0)$, which we consider constant over the measurement range (as discussed later), and a T-dependent thermal strain $\varepsilon_{bi}^{th}(T)$. To link the above relations with the variations observed for the Raman shift at different T, an accurate parametrization for the CTE as a function of the lattice temperature is also needed. Following Reeber and Wang,[34] we write $\alpha(T)$ as

$$\alpha_i = \sum_{i=1}^{n} X_i \frac{(\theta_i/T)^2 e^{(\theta_i/T)}}{\left[e^{(\theta_i/T)} - 1\right]^2} \tag{6}$$

where we use for the fitting parameters θ_i and X_i the ones in Reeber and Wang,[34] whose parametrization is also in good agreement with the one in Roucka et al.[35]

3 | EXPERIMENTAL METHODS AND RESULTS

Two intrinsic Ge/Si(001) samples (s_A and s_B) have been grown in a commercial reduced-pressure chemical vapor deposition reactor (RP-CVD, ASM Epsilon-2000). Standard Si(001) wafers are used as substrates; a first 50-nm-thick Ge buffer (seed) is deposited using N_2-GeH_4 at a growth rate of 5 nm/min. Subsequently, the wafer is heated up to 550 °C, and a 5-μm-thick Ge layer is deposited at a growth rate of 40 nm/min, resulting in a uniform thickness on the wafer. The deposition is followed by cyclic annealing up to T_{ann} = 850 °C for less than 20 min to decrease the defect density.[36] For s_A, cyclic annealing deposition is performed by interrupting the deposition process for several time intervals. For s_B, a conventional postannealing process is performed after the whole layer deposition. Because of this, the threading dislocation density, measured by the etch pit count method, results in 1×10^6 and $6 \times 10^6\ \text{cm}^{-2}$ for s_A and s_B, respectively.

Micro-Raman (μ-Raman) measurements at different T were carried out using a Renishaw inVia microscope in backscattering geometry using a 633-nm He—Ne laser for excitation (penetration depth in Ge ˜32 nm[37]), a 1,800 lines/mm grating, and a 50× objective (numerical aperture 0.75), resulting in a laser spot diameter of ˜0.8 μm. A liquid nitrogen Linkam cryostat was used to control the sample lattice temperature. The Raman shift was determined by performing a Voigt fit, which includes the measured width of the laser line. Data analysis follows the approach of Süess et al.[20] using standard statistical analysis, averaging on 11 sets of data acquired in different

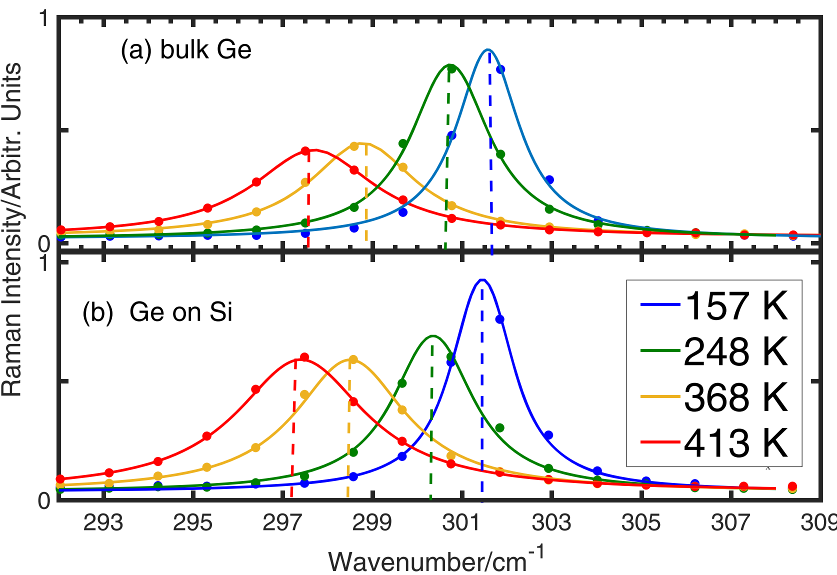

FIGURE 1 Raman spectra at different lattice temperature for bulk Ge(001; top panel) and Ge/Si sample s_A (bottom panel). Symbol and solid curves represent experimental data and Voigt fits, respectively [Colour figure can be viewed at wileyonlinelibrary.com]

positions of the sample to avoid laser heating and effects of strain inhomogeneities.

The reference is a cubic bulk Ge(001) sample, for which we obtained a Ge—Ge vibration mode wavenumber of 300.5 cm^{-1}, at room temperature.

In Figure 1, we show Raman spectra at different temperatures for the reference bulk Ge(001) crystal and for sample s_A. As the temperature increases from 150 to 413 K, the peak energy of the Ge bulk Ge—Ge Raman mode ω_0 decreases from 303.2 to 298.1 cm^{-1}, whereas its half width at half maximum (HWHM) increases from 0.83 to 1.9 cm^{-1} (see Figure 2). The observed trend for $\omega_0(Ge)$ is in agreement with both the Safran and Burke models[32,33] and with other experimental data reported in the literature [38–40]. Regarding the temperature behavior of the half width at half maximum in bulk Ge, the broadening of the Raman peak, and the subsequent decreasing in intensity with increasing temperature, is attributed to the temperature-dependent occupation number of phonon states and anharmonicity of the lattice.[32,33]

From Figure 2, it is clear that the Raman wavenumbers acquired on the epitaxial Ge/Si(001) have a T-dependence very similar to bulk Ge, albeit their values are systematically smaller. This effect is due to the presence of a biaxial strain field in the Ge/Si samples (see e.g., Capellini et al.[41]).

To relate the measured Raman shift with the T-dependence of the strain–shift coefficient $b(T)$, a precise evaluation of the strain magnitude ε as a function of the lattice temperature is required. For this purpose, we have performed HR-XRD experiments at different T. These were performed using a 9-kW SmartLab diffractometer from Rigaku in HR setup with Ge(400)×2 crystal collimator, Ge(220)×2 crystal analyzer, and CuK$_{\alpha 1}$ radiation (λ = 1.54059 Å). For high-temperature in situ experiments, a temperature control system from Anton Paar was mounted on the diffractometer, allowing to keep the

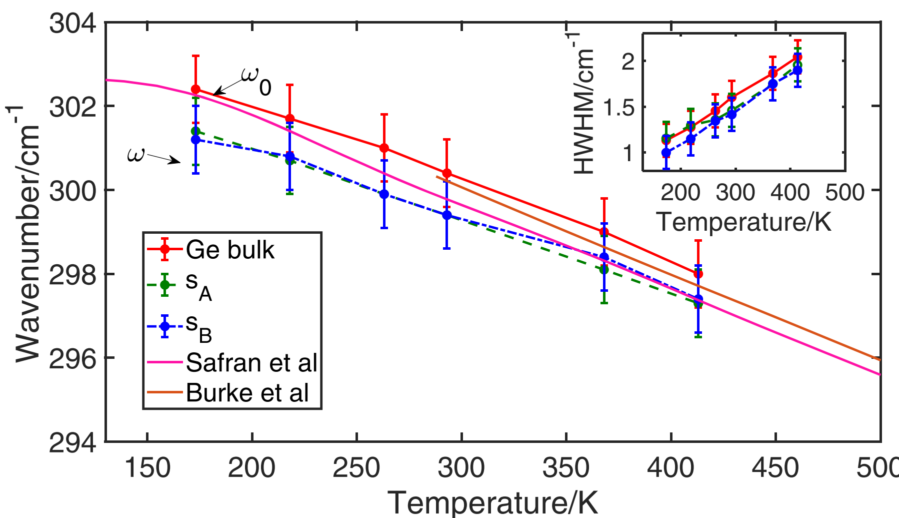

FIGURE 2 T-dependence of the Raman Ge—Ge mode peak position and half width at half maximum (HWHM; inset) in bulk Ge and heteroepitaxial Ge/Si samples.. For clarity, error bars are shown for selected data points only and determined from the statistical analysis of 11 data sets per each temperature. For comparison, Raman wavenumbers theoretically predicted by Safran et al.[32] and Burke et al.[33] in cubic Ge are also shown [Colour figure can be viewed at wileyonlinelibrary.com]

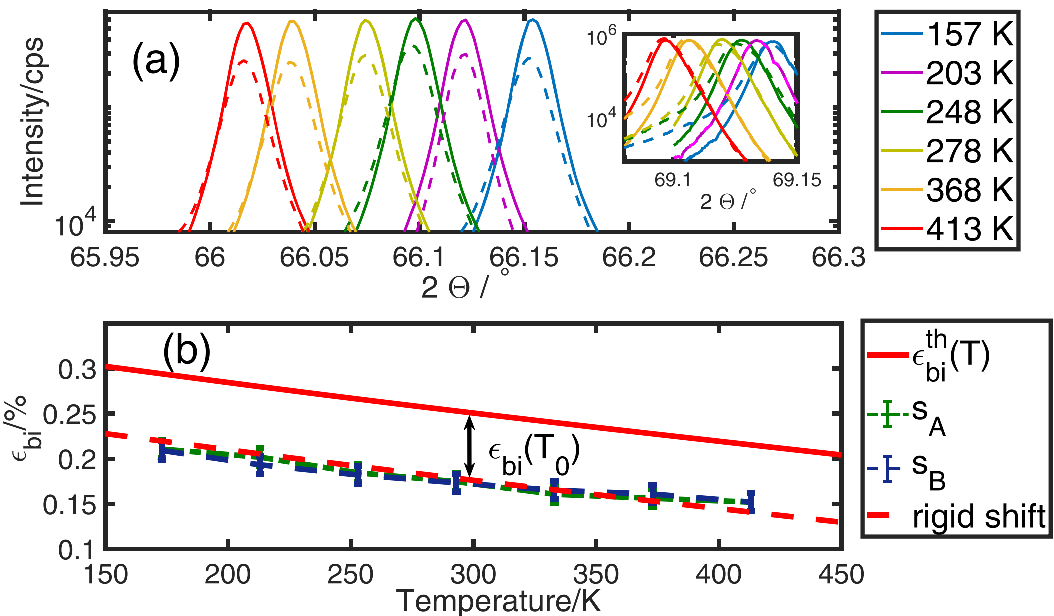

FIGURE 3 a) ω-2θ X-ray diffraction (XRD) scans around the (004) Ge diffraction acquired as a function of T on s_A (solid line) and s_B(dashed line). The Si reference is shown in the inset for each T. b) Resulting biaxial strain as a function of T in sample s_A(green dot–dashed curve) and s_B (blue dashed curve). The thermal strain $\varepsilon_{bi}^{th}(T)$, calculated according to Equation (5) having as a reference the annealing temperature $T_0 = 1123$ K is also shown (solid red curve). The red dashed curve has been obtained by a rigid shift of the $\varepsilon_{bi}^{th}(T)$ curve to estimate the $\varepsilon_{bi}(T_0)$ term [Colour figure can be viewed at wileyonlinelibrary.com]

samples in N_2 atmosphere while heated, and thus avoid oxidation and etching of the Ge layer. The Bragg peak position of the symmetrical (004) and asymmetrical (2-2-4) diffractions of both the Si substrate and the Ge epilayer were measured at room temperature to obtain in-plane and out-of-plane lattice parameters, respectively. The modification of Ge in-plane lattice parameter follows the one of Si, measured by (004) peak position (inset in Figure 3a), with no change of relaxation expected in the range 157–413 K. The measurement of the off-plane lattice parameter of Ge, by the corresponding (004) reflection of Figure 3a, provides the in-plane lattice parameter of Ge from well-known elastic relations.

The obtained data show a monotonic decrease of $\varepsilon_{bi}(T)$ for increasing T, almost identical in samples s_A and s_B (Figure 3b). The red solid curve in Figure 3b, calculated according to Equations (5) and (6) using $T_0 = T_{ann} = 1123\ K$, represents the thermal contribution to the biaxial strain $\varepsilon_{bi}^{th}(T)$. The difference between the calculated $\varepsilon_{bi}^{th}(T)$ and the measured ε_{bi} values remains constant within the experimental uncertainty over the explored T range. For clarity, this is highlighted by the dashed curve in Figure 3b, obtained by a rigid translation of the $\varepsilon_{bi}^{th}(T)$ data by an amount $\varepsilon_{bi}(T_0)$, that is, by the heteroepitaxial strain contribution to the overall strain field. As expected, $\varepsilon_{bi}(T_0)$ is temperature-independent, and its value of -7.5×10^{-4} is in very good agreement with previous findings.[41] We point here out that our measurement procedure for $\varepsilon_{bi}(T_0)$ relies on the implicit assumption of complete hardening of the dislocation networks in the Ge/Si epilayer after the annealing treatment. In other words, the motion and reactions of the threading dislocations after the postgrowth annealing, that is, during the measurement process, would further lower the $\varepsilon_{bi}(T_0)$ value.[37] However, in our system, we can rule this out as the T-dependent measurements have been carried out at T much lower (<450 K) than the annealing one (T_0=1,123 K).

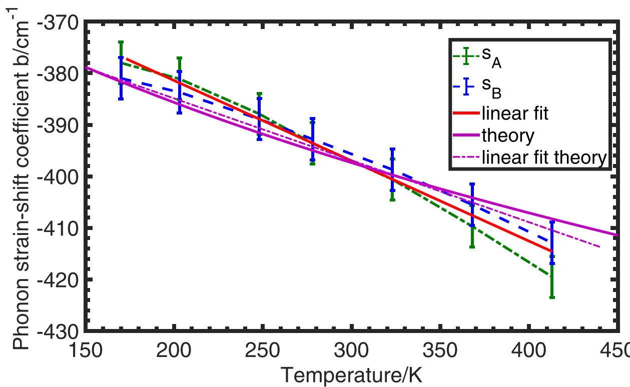

FIGURE 4 Measured strain–phonon coefficient in epitaxial Ge as a function of T for sample s_A (dashed blue) and s_B (dot dashed green); the red solid line represents a linear fit whereas the magenta solid curve has been obtained from Equation (3) as discussed in the text; its linear fit is reported in dashed magenta [Colour figure can be viewed at wileyonlinelibrary.com]

TABLE 1 Strain–phonon coefficient and corresponding excitation wavelength and experimental conditions reported in the literature. All acquired in μ-Raman setups in backscattering geometry

Reference	Strain–phonon coefficient *b*	Excitation wavelength	Material
	(cm^{-1})	(nm)	
This work	−395	633	Ge on SOI
Capellini et al.[8]	−390	633	Ge/Si (001)
Reparaz. et al.[21]	−460 ± 20	514	SiGe alloys
Cerdeira et al.[24]	−455	488	GeSi/Si strained superlattice
Pezzoli et al.[44]	−450 ± 20	488, 458, 364	SiGe alloy
Gassenq et al.[45]	−455	785	Ge
Lockwood et al.[23]	−408	458	SiGe alloy
Rouchon et al.[43]	−403 ± 90	514	Ge
Perova et al. [46]	−384	488, 457, 325	SiGe alloys

4 | DISCUSSION

In Figure 4 (magenta curve), we show the T-dependent behavior of the strain–shift coefficient $b(T)$ calculated using Equation (3). We observe a monotonic decrease with values ranging between −380 and −420 cm^{-1} for T increasing in the 150–413 K range. This behavior is mainly to be attributed to T-induced decrease of the Raman shift ω_0, with the variation of the c_{12}/c_{11} ratio giving a lesser contribution, considering the values of PDPs of Peng et al. [23]

This theoretical curve is compared with experimental results obtained on both s_A and s_B samples, by using in Equation (1) the measured Raman shifts and the strain values obtained by XRD (blue dashed and green dot–dashed curves in Figure 4). A linear fit (solid red curve in Figure 4) of these experimental data gives for $b(T)$

$$b\left(\mathrm{cm}^{-1}\right) = -0.15 \pm 0.03\left(\frac{\mathrm{cm}^{-1}}{\mathrm{K}}\right)T(\mathrm{K}) - 350 \pm 8\left(\mathrm{cm}^{-1}\right) \quad (7)$$

in good agreement with our theoretical estimation obtained from Equation (3). Indeed, the linear fit of the theoretical equation is giving a value for the slope db(T)/dT = −0.13(cm^{-1}/K; purple dashed line in Figure 4). We also notice the good match existing between the experimental and theoretical values of b (RT) = −395 cm^{-1}, which is also in very good agreement with the theoretical prediction reported in Pezzoli et al.[42]. Nevertheless, measurements of b at 300 K reported in the literature are quite scattered, ranging from a minimum of −460 cm^{-1} [21] to a maximum of −384 cm^{-1} [43], as shown in Table 1.

This large uncertainty interval might be attributed to (a) the limited accuracy associated to the evaluation of the strain field when the epilayer features an inhomogeneous strain profile or by techniques different from HR-XRD; and (b) heating effects associated to the optical excitation of the samples. Moreover, as reported in Table 1, several experiments have been carried out with SiGe samples, extrapolating the strain–phonon coefficient for Ge in the limit of zero Si content. In this case, an overestimation of the absolute value of the Ge strain–phonon coefficient is systematically obtained. Concerning the strain measurements, it is worth noting that, while the XRD probes the average strain within the epilayer, the Raman technique, especially when carried out using a short excitation wavelength, is more surface-sensitive, owing to the limited penetration length of the pump radiation. This can alter the results when thin and/or lithographically defined samples are investigated (see e.g., Capellini et al.[6] and Chahine et al.[47]) because the lattice usually features a complex strain distribution along the vertical and/or lateral directions.[6,47] As an example, we can estimate from our results that an uncertainty in the measurement of ε_{bi} of the order of 0.1% reflects in a corresponding variation for b of ~15 cm^{-1}. On the other hand, the limited penetration depth in Ge of conventionally used laser sources for μ-Raman, together with the use of high magnification objective, might bring a rather high optical power density on the sample surface, inducing local heating. In this case, from Figure 4, we can see that a local difference in lattice T of 50 K can entail a change in b as large as ~10 cm^{-1}.

5 | CONCLUSIONS

In summary, we have investigated the temperature dependence of the strain–shift coefficient in Ge layers. To this aim, a proper theoretical framework has been developed and used to interpret experimental data obtained

from μ−Raman and HR-XRD experiments, performed with Ge samples whose lattice temperature was varied in the 150 to 413-K interval. Upon increasing T, a monotonic decrease of $b(T)$, with a slope of -0.15 ± 0.03 cm^{-1}/K, well matches with our theoretical prediction. As a byproduct of this investigation, also, the temperature dependence of the biaxial strain field in this T range has been fully characterized.

The accurate estimation of the strain–phonon coefficient in a wide range of temperatures presents an applicative relevance for the development of optoelectronic devices based on strained Ge layers and operating at different temperatures.

ACKNOWLEDGEMENTS

This work is supported by the European Union research and innovation program Horizon 2020 under Grant No. 766719–FLASH Project.

ORCID

C.L. Manganelli https://orcid.org/0000-0002-4218-2872
D. Spirito https://orcid.org/0000-0002-6074-957X

REFERENCES

[1] D. Liang, J. E. Bowers, *Nat. Phot.* **2010**, *4*, 511.
[2] R. Soref, *IEEE J.Sel. Top. Quant. Elect.* **2006**, *12*, 1678.
[3] J. Michel, J. Liu, L. C. Kimerling, *Nature Photonics* **2010**, *4*, 527.
[4] J. Liu, X. Sun, R. Camacho-Aguilera, L. C. Kimerling, J. Michel, *Opt. Lett.* **2010**, *35*, 679.
[5] R. E. Camacho-Aguilera, Y. Cai, N. Patel, J. T. Bessette, M. Romagnoli, L. C. Kimerling, J. Michel, *Opt. Expr.* **2012**, *20*, 11316.
[6] G. Capellini, C. Reich, S. Guha, Y. Yamamoto, M. Lisker, M. Virgilio, A. Ghrib, M. El Kurdi, P. Boucaud, B. Tillack, *Opt. Expr.* **2014**, *22*, 399.
[7] J. Liu, R. Camacho-Aguilera, J. T. Bessette, X. Sun, X. Wang, Y. Cai, L. Kimerling, J. Michel, *Thin Solid Films* **2012**, *520*, 3354.
[8] G. Capellini, G. Kozlowski, Y. Yamamoto, M. Lisker, C. Wenger, G. Niu, P. Zaumseil, B. Tillack, A. Ghrib, M. De Kersauson, *J. Appl. Phys.* **2013**, *113*, 013513.
[9] G. Shambat, S. L. Cheng, J. Lu, Y. Nishi, J. Vuckovic, *Appl. Phys. Lett.* **2010**, *97*, 241102.
[10] M. Virgilio, C. L. Manganelli, G. Grosso, G. Pizzi, G. Capellini, *Phys.Rev. B* **2013**, *87*, 235313.
[11] J. Liu, X. Sun, D. Pan, X. Wang, L. C. Kimerling, T. L. Koch, J. Michel, *Opt. Expr.* **2007**, *15*, 11272.
[12] F. Montalenti, M. Salvalaglio, A. Marzegalli, P. Zaumseil, G. Capellini, T. U. Schülli, M. A. Schubert, Y. Yamamoto, B. Tillack, T. Schroeder, *Phys. Rev. B* **2014**, *89*, 014101.
[13] F. Isa, M. Salvalaglio, Y. A. R. Dasilva, M. Meduna, M. Barget, A. Jung, T. Kreiliger, G. Isella, R. Erni, F. Pezzoli, E. Bonera, P. Niedermann, P. Groning, F. Montalenti, H. von Kanel, *Adv. Material* **2016**, *2*, 5.
[14] K. Sawano, Y. Abe, H. Satoh, *Appl. Phys. Lett* **2005**, *87*, 192102.
[15] M. Salvalaglio, P. Zaumseil, Y. Yamamoto, O. Skibitzki, R. Bergamaschini, T. Schroeder, A. Voigt, G. Capellini, *Appl. Phys. Lett.* **2018**, *112*, 022101.
[16] T. Beechem, A. Christensen, S. Graham, D. Green, *J. Appl. Phys.* **2008**, *103*, 124501.
[17] T. Beechem, A. Christensen, S. Graham, *Rev. Sci.. Instr.* **2007**, *78*, 061301.
[18] B. S. Williams, *Nat. Phot.* **2007**, *1*, 517.
[19] F. Schaffler, *Semicond. Sci. Technol.* **1997**, *12*, 1515.
[20] M. J. Süess, R. A. Minamisawa, R. Geiger, K. K. Bourdelle, H. Sigg, R. Spolenak, *Nanolett.* **2014**, *14*, 1249.
[21] J. Reparaz, A. Bernardi, A. Goni, M. Alonso, M. Garriga, *Appl. Phys. Lett.* **2008**, *92*, 081909.
[22] S. Ganesan, A. Maradudin, J. Oitmaa, *Annals of Phys.* **1970**, *56*, 556.
[23] C. Y. Peng, C.-F. Huang, Y. C. Fu, Y.-H. Yang, C.-Y. Lai, S.-T. Chang, C. W. Liu, *J. Appl. Phys.* **2009**, *105*, 083537.
[24] F. Cerdeira, M. Cardona, *Phys. Rev. B* **1972**, *5*, 1440.
[25] T. Etzeldorfer, A. Wyss, M. J. Suess, F. F. Schlich, R. Geiger, J. Frigerio, J. Stangl, *Meas. Sci. Technol.* **2017**, *28*, 025501.
[26] E. Anastassakis, E. Burstein, *J. Phys. Chem. Solids* **1971**, *2*, 563.
[27] F. Cerdeira, C. J. Buchenauer, F. H. Pollak, M. Cardona, *Phys. Rev. B* **1972**, *5*, 580.
[28] Z. Sui, I. P. Herman, *Phys. Rev. B* **1993**, *48*, 24.
[29] E. Anastassakis, A. Cantarero, M. Cardona, *Phys. Rev. B* **1991**, *41*, 11.
[30] H. Rucker, M. Methfessel, *Phys. Rev. B* **1995**, *52*, 15.
[31] H. J. McSkimin, *J. Appl. Phys.* **1953**, *24*, 988.
[32] S. Safran, S. Lax, *J. Phys. Chem. Solids* **1975**, *36*, 753.
[33] H. Burke, I. P. Herman, *Phys. Rev. B.* **1993**, *48*, 15016.
[34] R. Reeber, K. Wang, *Mat. Chem. Phys.* **1996**, *46*, 259.
[35] R. Roucka, Y. Y. Fang, J. Kouvetakis, A. V. G. Chizmeshya, J. Menéndez, *Phys. Rev. B* **2010**, *81*, 245214.
[36] Y. Yamamoto, P. Zaumseil, M. A. Shubert, B. Tillack, *Semicond Sci. Tecnol.* **2018**, *33*, 124007.
[37] J. Jimenez, J. W. Tomm, *Spectroscopic Analysis of Optoelectronic Semiconductors*, Springer International Publishing, Switzerland **2016**.
[38] M. Cardona, R. Merlin, *Light Scattering in Solid IX*, Springer, Berlin **2006**.
[39] P. G. Klemens, *Phys. Rev.* **1966**, *148*, 845.
[40] R. A. Cowley, *J. Phys.* **1965**, *26*, 659.
[41] G. Capellini, M. De Seta, P. Zaumseil, G. Kozlowski, T. Schroeder, *J. Appl. Phys.* **2012**, *111*, 073518.
[42] F. Pezzoli, E. Grilli, M. Guzzi, S. Sanguinetti, D. Chrastina, G. Isella, H. von Känel, E. Wintersberger, J. Stangl, G. Bauer, *Mater. Sci. Semicond. Process.* **2006**, *9*, 541.
[43] D. Rouchon, M. Mermoux, F. Bertin, J. Hartmann, *J. Cryst. Growth* **2014**, *392*, 66.
[44] F. Pezzoli, E. Bonera, E. Grilli, E. Guzzi, M. Sanguinetti, D. Chrastina, G. Isella, H. Von Känel, E. Wintersberger, J. Stangl, *J. Appl. Phys.* **2008**, *103*, 093521.
[45] A. Gassenenq, S. Tardif, K. Guilloy, I. Duchemin, N. Pauc, J. M. Hartmann, D. Rouchon, J. Widiez, Y. M. Niquet, L. Milord, T. Zabel, H. Sigg, J. Faist, A. Chelnokov, F. Rieutord, V. Reboud, V. Calvo, *J. Appl. Phys.* **2017**, *121*, 055702.

[46] T. Perova, J. Wasyluk, K. Lyutovich, E. Kasper, M. Oehme, K. Rode, A. Waldron, *J. Appl. Phys.* **2011**, *109*, 03350.
[47] G. A. Chahine, M. H. Zoellner, M.-I. Richard, S. Guha, C. Reich, P. Zaumseil, G. Capellini, T. Schroeder, T. U. Schülli, *Appl. Phys. Lett.* **2015**, *106*, 071902.

SUPPORTING INFORMATION

Additional supporting information may be found online in the Supporting Information section at the end of this article.

How to cite this article: Manganelli CL, Virgilio M, Skibitzki O, et al. Temperature dependence of strain–phonon coefficient in epitaxial Ge/Si(001): A comprehensive analysis. *J Raman Spectrosc*. 2020;51:989–996. https://doi.org/10.1002/jrs.5860